

IL NUOVO CIMENTO  
DOI 10.1393/ncc/i2012-11360-0

VOL. 35 C, N. 6

Novembre-Dicembre 2012

COLLOQUIA: LaThuile12

## Recent QCD studies at the Tevatron

S. MOED SHER

*Fermilab - Batavia, IL, USA*

ricevuto il 7 Settembre 2012

**Summary.** — Since the beginning of Run II at the Fermilab Tevatron, the QCD physics groups of the CDF and D0 Collaborations have worked to reach unprecedented levels of precision for many QCD observables. This note summarizes important recent measurements with dataset corresponding to up to  $8 \text{ fb}^{-1}$  of total integrated luminosity.

PACS 12.38.-t – Quantum chromodynamics.

### 1. – Introduction

The Tevatron collider at Fermilab provides collisions of protons with anti-protons at a center-of-mass energy of 1.96 TeV. By the end of the Tevatron Run II, the multipurpose detectors of the CDF [1] and D0 [2] experiments were delivered a total integrated luminosity of about  $12 \text{ fb}^{-1}$ . This large amount of data is exploited in order to make important progress in constraining and confirming the calculations of quantum chromodynamics (QCD) theory. Precise measurements of QCD observables in hadron-hadron collisions, such as jet cross sections, constrain parton density functions (PDFs) and confirm the predictive power of theory. This results in a better control of the standard QCD production calculations, which are used to predict major backgrounds for many important physical processes. In addition, the specific QCD processes which pose challenges to New Physics searches such as supersymmetry and Higgs production can be measured directly with the increased size of available datasets.

In this note some of the recent measurements from the CDF and D0 Collaborations are reviewed. These measurements are related to QCD hard scattering processes. A brief introduction to the structure of hadronic collisions is useful as a motivation for jet definition. Hadronic collision may be factorized into perturbative components (hard scattering and initial and final state radiation) and non-perturbative components (beam remnants and multiple parton interactions). These components are illustrated in fig. 1.

This simple picture is an example of processes which are modeled by Monte Carlo generating programs to simulate hadronic collisions. The picture becomes more complicated when the properties of QCD color confinement and detector effects are included.

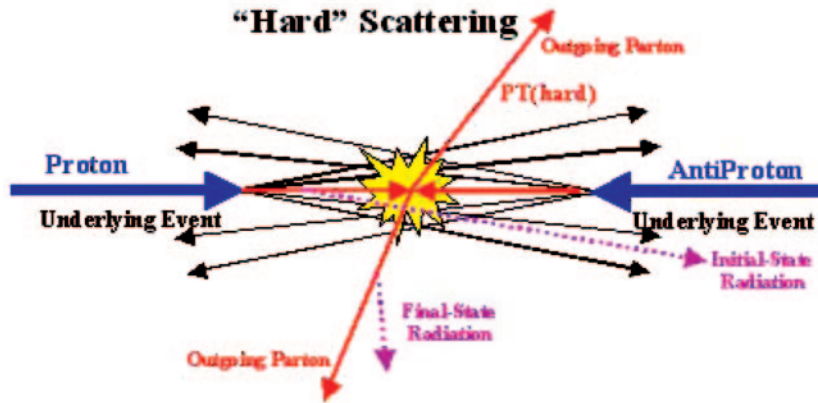


Fig. 1. – Simple model for hadronic collisions.

The colored partons must hadronize into color neutral hadrons. These particles are then clustered into jets by jets algorithms. Jets may be clustered at the parton (quarks and gluons), particle (hadrons) or detector (calorimeter towers) level. Measurements are made at the detector level, but it is useful to use the parton and particle level jets from Monte Carlo simulations to derive corrections to the measured quantities.

The analyses discussed in this note focus on the perturbative component of the collision and do not include studies of the non-perturbative regime (where pQCD fails), such as the “soft” interactions generating the underlying event which accompanies the “hard” collision.

## 2. – Angular decorrelations in $\gamma + 2(3)$ jets

The D0 Collaboration used inclusive  $\gamma + 2$  jets and  $\gamma + 3$  jets events with an integrated luminosity of about  $1\text{fb}^{-1}$  to measure cross sections as a function of the angle in the plane transverse to the beam direction between the transverse momentum ( $P_T$ ) of the  $\gamma +$  leading jet system (jets are ordered in  $P_T$ ) and the  $P_T$  of the other jet for the  $\gamma + 2$  jet events, or  $P_T$  sum of the two other jets for the  $\gamma + 3$  jet events, [3]. Differential cross sections were studied in three bins of the second jet  $P_T$ . The results are compared to different Multiple Parton Interaction (MPI) models and demonstrate that the prediction of the Single Particle (SP) models do not describe the measurements, and an additional contribution from Double Parton (DP) events is required to describe the data. The data favors the predictions of the new PYTHIA MPI models with  $P_T$ -ordered showers, implemented in the Perugia and S0 tunes, and also SHERPA with its default MPI model. Predictions from previous PYTHIA MPI models with tunes A and DW are disfavored. The results of these measurements are shown in fig. 2.

## 3. – Three jet mass cross section

Using about  $0.7\text{fb}^{-1}$  of integrated luminosity collected by the D0 experiment, differential cross sections for three jet mass were measured, [4]. In this measurement jets are defined by the midpoint cone algorithm with cone size  $R = 0.7$ . Five scenarios were considered, where the rapidities of the three leading  $P_T$  jets are restricted to  $|y| < 0.8$ ,  $|y| < 1.6$ ,  $|y| < 2.4$ . The transverse momentum selection required  $P_{T1} > 150\text{GeV}/c$ , and

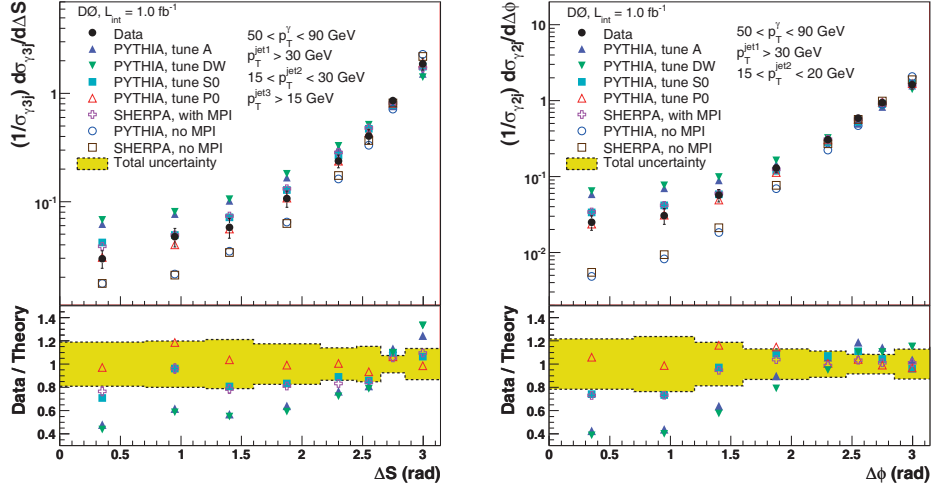


Fig. 2. – On the left: normalized differential cross section in  $\gamma+3$  jet events,  $(1/\sigma_{\gamma 3j})d\sigma_{\gamma 3j}/d\Delta S$ , in data compared to MC models, and the ratio of data over theory, only for models including MPI, in the range  $15 < P_T^{jet2} < 30$  GeV. On the right: normalized differential cross section in  $\gamma+2$  jet events,  $(1/\sigma_{\gamma 2j})d\sigma_{\gamma 2j}/d\Delta\phi$ , in data compared to MC models, and the ratio of data over theory, only for models including MPI, in the range  $15 < P_T^{jet2} < 20$  GeV.

$P_{T3} > 40$  GeV/c. For  $|y| < 2.4$  additional measurements are made for  $P_{T3} > 70$  GeV and  $P_{T3} > 100$  GeV. Figure 3 shows results for the differential three jet cross section in  $M_{3j}$ , for different rapidity ranges and for different  $P_T$  criteria. The data are compared to theoretical models of NLO pQCD and non-perturbative corrections. The renormalization and factorization scales are set to the average  $P_T$  of the three leading  $P_T$  jets:  $\mu_R = \mu_F = \mu_0 = (P_{T1} + P_{T2} + P_{T3})/3$ . Figure 4 shows the ratio between data and theory

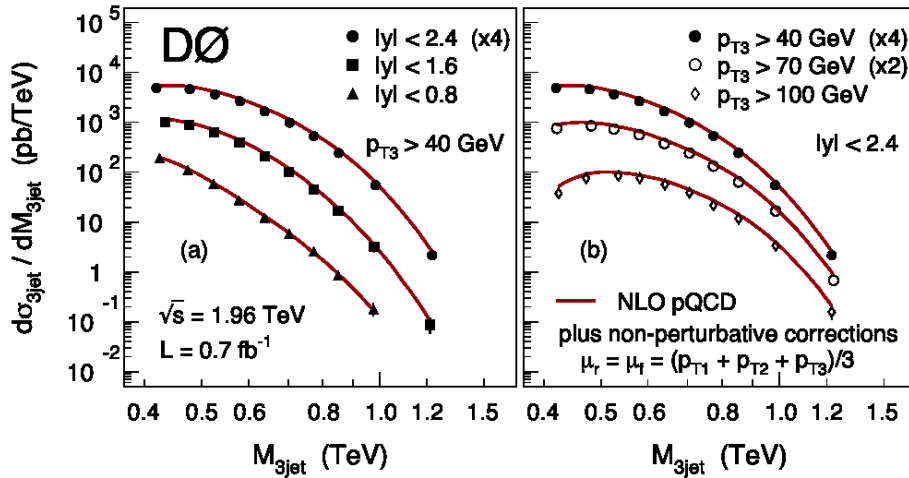


Fig. 3. – D0 measurement of the three-jet cross section as a function of the three-jet invariant mass in different rapidity regions (left) and for different  $P_{T3}$  requirements (right).

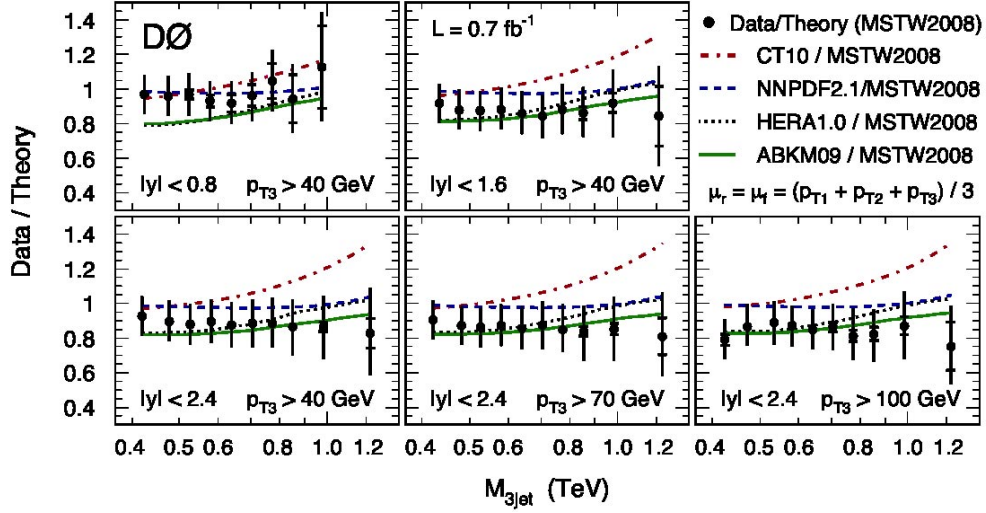


Fig. 4. – Ratios between data and theory for the D0 three-jet cross section measurement. The ratios are computed for different PDFs and are shown as a function of the three-jet invariant mass in different rapidity regions and for different  $P_{T3}$  requirements.

for different PDFs. The data are reasonably well described by the next-to-leading order calculation done with NLOJET++ and the MSTW2008NLO PDFs.

#### 4. – $W + \text{jets}$ production

The measurements of inclusive  $W(\rightarrow e\nu) + n$  jets cross sections ( $n = 1, 2, 3, 4$ ), presented as total inclusive cross sections and differentially in the  $n$ -th jet transverse momentum was done by the D0 Collaboration [5]. The measurements are made using data corresponding to an integrated luminosity of  $4.2 \text{ fb}^{-1}$ . The selection for  $W + n$  jet events include the following criteria: presence of a central electron with  $P_T > 15 \text{ GeV}$ , missing transverse energy  $> 20 \text{ GeV}$ , transverse mass of the  $W$  boson candidate  $> 40 \text{ GeV}/c$ , and the jet transverse momentum  $> 20 \text{ GeV}$ . The spatial distance between the cone and the nearest jet is required to be  $\Delta R > 0.5$ . Acceptance corrections and background contributions from  $Z + \text{jets}$ , top pair production, diboson and single top production are estimated using different MC events generators [5]. The backgrounds from multijet production are determined using a data driven method. Figure 5 shows these cross section results as a function of  $P_T$  of the first, second, third and fourth jet, and compared to pQCD predictions in NLO (for  $n_{jet} < 3$ ) or LO (for  $n_{jet} = 4$ ). Within their uncertainties, the NLO pQCD predictions agree pretty well with the data, except for the low  $P_T$  region for  $W + 1$  jet and high- $P_T$  region for  $W + 3$  jets. The LO predictions for  $W + 4$  jets agree with the data, but have very large uncertainties from the renormalization scale dependence.

#### 5. – Observation of $W$ boson + single-charm production

Calculations of  $W + \text{heavy quark}$  production are available at leading order (LO) and next-to-leading order (NLO) QCD [6], with the NLO cross section about 50% larger than

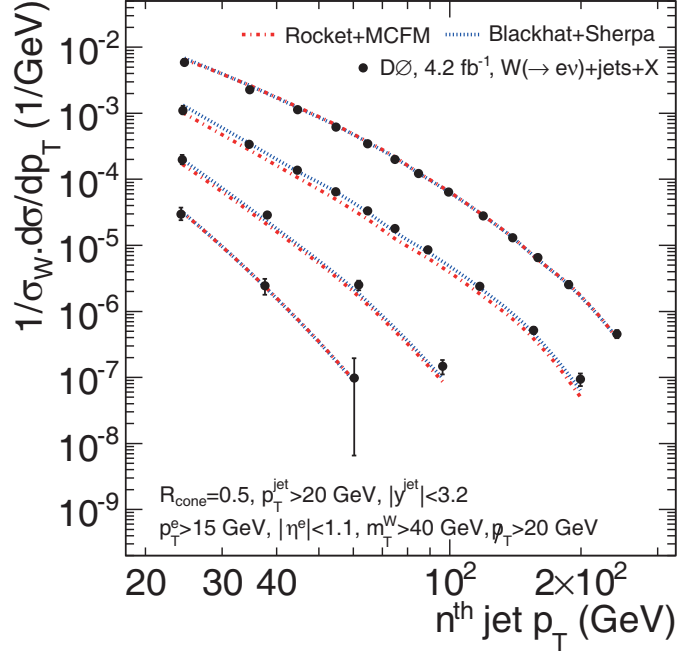


Fig. 5. – Measured  $W + n$  jet differential cross section as a function of  $n$ -th jet  $P_T$  for jet multiplicities  $n = 14$ , normalized to the inclusive  $W \rightarrow e$  cross section.  $W + 1$  jet inclusive spectra are shown by the top curve, the  $W + 4$  jet inclusive spectra by the bottom curve. The measurements are compared to the fixed-order NLO predictions for the jet multiplicities  $n = 13$ , and to LO predictions for  $n = 4$ .

at LO. Overall, the uncertainty on the NLO theoretical expectation for  $W$  boson + single-charm quark production at the Tevatron is about 1020%, depending on the charm phase space, with the largest uncertainties due to the choice of factorization and renormalization scales and the shape of the  $s$  quark PDF.

The CDF Collaboration performed the first observation of the  $p\bar{p} \rightarrow Wc$  production cross section at the Tevatron collider [7]. The charm quark is identified through the semileptonic decay of the charm hadron into an electron or muon (soft leptons). The  $Wc$  production cross section is determined first separately using soft electrons and soft muons, and then the two measurements are combined. The analysis exploits the correlation between the charge of the  $W$  boson and the charge of the soft lepton from the semileptonic decay of the charmed hadron. Charge conservation in the process  $gq \rightarrow Wc$  ( $q = d, s$ ) allows as final states only the pairings  $W^+\bar{c}$  and  $Wc$ ; as a result, the charge of the lepton from the semileptonic decay of the  $c$  quark and the charge of the  $W$  boson are always of opposite sign. In practice, this correlation is diluted in the reconstructed events due to hadronic decays in flight and hadrons misidentified as soft leptons. These contaminations in the signal selection and other background contributions, such as  $W +$  jets and  $Z +$  jets production, top pair production and single top, as well as diboson and multijet production, are considered in the analysis. The  $W$  is identified through its leptonic decay. The measured production cross section  $\sigma_{Wc}(P_{Tc} > 20 \text{ GeV}/c, |\eta_c| < 1.5) - B(W \rightarrow l\nu) = 13.3 + 3.3 \text{ pb}$ , in agreement with theoretical expectations, with a significance for the  $Wc$  signal of  $6.4\sigma$ .

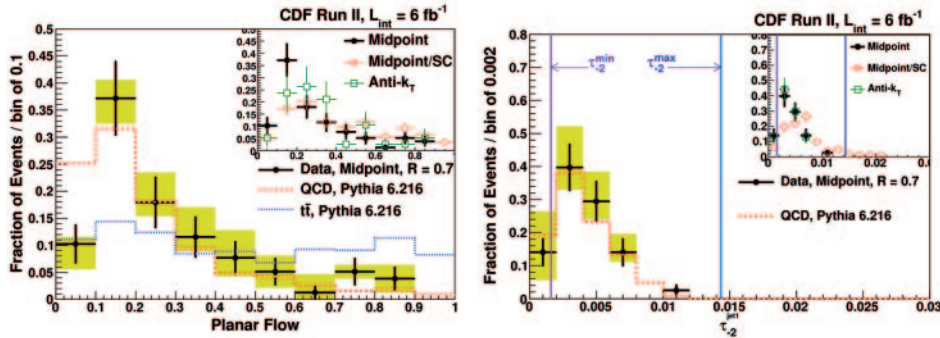


Fig. 6. – The angularity distribution for midpoint jets with  $P_T > 400 \text{ GeV}/c$ . The  $t\bar{t}$  rejection cuts and requirement for  $90 \text{ GeV} < m_{j1} < 120 \text{ GeV}$  are applied. The PYTHIA calculation (red dashed line) and the pQCD kinematic endpoints are shown (left); The planar flow distributions after applying the top rejection cuts and requiring  $130 \text{ GeV} < m_{j1} < 210 \text{ GeV}$ . PYTHIA QCD (red dashed line) and  $t\bar{t}$  (blue dotted line) jets are shown (right).

## 6. – Jet substructure

The study of high-transverse-momentum massive jets provides an important test of pQCD and gives an insight into the parton showering mechanism. In addition, massive boosted jets compose an important background in searches for various new physics models, the Higgs boson, and highly boosted top quark pair production. Particularly relevant is the case where the decay of a heavy resonance produces high- $P_T$  top quarks that decay hadronically. In all these cases, the hadronic decay products can be detected as a single jet with substructure that differs from pQCD jets once the jet  $P_T$  is greater than 400–500  $\text{GeV}/c$ . The CDF Collaboration performed a measurement of substructure of jets with  $P_T > 400 \text{ GeV}/c$  by studying distributions of the jet mass and measuring angularity, the variable describing the energy distribution inside the jet, and planar flow, the variable differentiating between two-prong and three-prong decays [8]. At small cone sizes and large jet mass, these variables are expected to be quite robust against soft radiation and allow, in principle, a comparison with theoretical predictions in addition to comparison with MC results. Jets are reconstructed with the midpoint cone algorithm (cone radii  $R = 0.4, 0.7,$  and  $1.0$ ) and with the antikt algorithm [9] (with distance parameter  $R = 0.7$ ). Events are selected in a sample with  $6 \text{ fb}^{-1}$  based on the inclusive jet trigger. There is a good agreement between the measurement and the analytic predictions and with PYTHIA MC predictions. The midpoint and antikt algorithms have very similar jet substructure distributions for high mass jets, see fig. 6. The angularity distribution shown on fig. 6 (left) in addition to reasonable agreement data and PYTHIA MC also demonstrates that the high-mass jets coming from light quark and gluon production are consistent with two-body final states and that further rejection against high mass QCD jets can be obtained by using the planar flow variable, fig. 6 (right).

## 7. – Conclusions

Measurements from the Tevatron Run II defined a new level of QCD precision measurements in hadron-hadron collisions. Several results from the Tevatron were reviewed in this note mostly showing nice agreement with NLO predictions. The QCD programs of

the CDF and D0 Collaborations have been dedicated to testing and constraining pQCD and also measuring cross sections of important background processes. These studies are important for many searches at the Large Hadron Collider (LHC), where measurements of this type are among the first to be made using LHC data [10,11].

## REFERENCES

- [1] ACOSTA D. E. *et al.* (CDF COLLABORATION), *Phys. Rev. D*, **71** (2005) 032001.
- [2] LECOMPTE T. and DIEHL H. T., *Ann. Rev. Nucl. Part. Sci.*, **50** (2000) 71.
- [3] ABAZOV V. M. *et al.* (D0 COLLABORATION), *Phys. Rev. D*, **83** (2011) 052008.
- [4] ABAZOV V. M. *et al.* (D0 COLLABORATION), arXiv:1104.1986v2 [hep-ex] (2011).
- [5] ABAZOV V. M. *et al.* (D0 COLLABORATION), *Phys. Lett. B*, **705** (2011) 200.
- [6] KELLER S., GIELE W. T. and LAENEN E., *Phys. Lett. B*, **372** (1996) 141.
- [7] CDF COLLABORATION, *Public note*, <http://www-cdf.fnal.gov/physics/new/qcd/QCD.html> (2012).
- [8] AALTONEN T. *et al.* (CDF COLLABORATION), arXiv:1106.5952v2 [hep-ex] (2011).
- [9] CACCIARI S. G. P. and SOYEZ G., *JHEP*, **04** (2008) 063.
- [10] CMS COLLABORATION, *CERN-CMS-NOTE-2006*, **067** (2007) .
- [11] SKANDS P. Z., *Contribution to Les Houches Workshop on Physics at TeV Colliders* FERMILAB-CONF-07-706-T (2007).